LOW-VOLTAGE FERROELECTRIC PHASE SHIFTERS FROM L- TO C-BAND

J. Stevenson Kenney[1], Yong Kyu Yoon[1], Minsik Ahn[1], Mark G. Allen[1], Zhiyong Zhao,[2] Xiaoyan Wang,[2] Andrew Hunt[2], and Dongsu Kim[3]
[1]School of Electrical and Computer Engineering, Georgia Institute of Technology, Atlanta, GA, USA
[2] *n*Gimat Inc., 5315 Peachtree Industrial Blvd, Atlanta, GA, USA
[3]Korean Electronics Technology Institute, Seoul, Korea

Abstract—This paper describes the design, fabrication and test results of a family of integrated low voltage ferroelectric phase shifters ranging in frequency of operation from 0.7 GHz to 6 GHz. All devices use a common material system of $Ba_xSr_{1-x}TiO_3$ (BST) thin-films on Al_2O_3 (sapphire), allowing integration with high-Q inductors and other passive microwave elements. Novel bias structures have also been developed to reduce the voltages required to tune the materials, making them more attractive for avionics systems applications.

I. INTRODUCTION

Ferroelectric materials, due to their low loss, high power handling capability, and wide range of tunable dielectric constant, have attracted much attention for tunable microwave device applications over the past decade. However, their insertion into modern avionics systems has been hindered by the high voltages required to tune the dielectric constant. This paper describes innovations in materials, deposition processes, and circuit design techniques that have overcome such system level limitations. Potential applications of interest in avionics are also examined.

II. FERROELECTRIC MATERIALS

Ferroelectric materials have been studied for half a century now, and the material properties of many such compounds are quite well known [1]. All ferroelectric materials have a similar characteristic that an asymmetry can exist within the unit cell that gives rise to a static polarization below a critical temperature, called the Currie temperature (T_c). Figure 1 shows the molecular structure of $Ba_xSr_{1-x}TiO_3$ or "BST." Below the T_c, the Ti atom is offset from the plane of O atoms, giving rise to a local polarization. As is seen from Figure 1, the location of the Ti may be above, or below the plane in either direction. Hence no net polarization occurs within a bulk sample. However, if an external static electric field is applied in a favorable direction, the Ti atoms will align, and remain in that orientation after the field is removed. This remnant polarization is illustrated in the *P-E* curve shown on the lower left side of Figure 2.

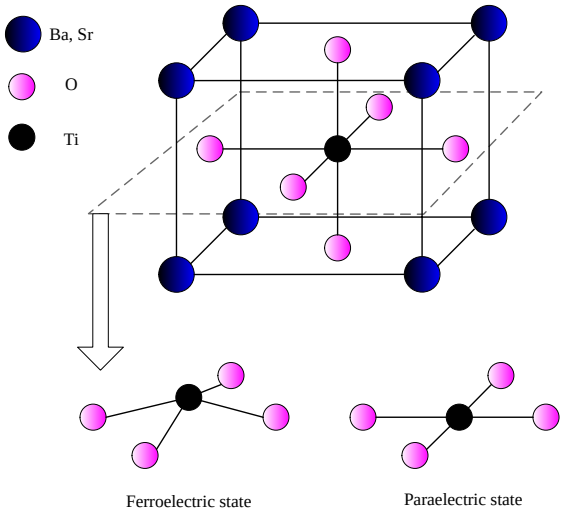

Figure 1: Unit cell of barium-strontium-titanate (BST) in ferroelectric and paraelectric states.

Ferroelectric materials have found applications in nonvolatile memories, but are of limited interest for microwave applications [2]. The primary reason is that energy is lost to the material over each cycle as the *E*-field traverses around the *P-E* contour. In contrast to the ferroelectric state, a paraelectric state also exists above the Currie temperature. Above this temperature, the Ti atom relaxes to the center of the unit cell with little remnant polarization. The molecule is still strongly polar, as the location of the Ti atom, and hence the dipole moment, may be easily shifted with the application of an external E-field. Not only does this give rise to a high relative permeability (ε_r), but along a nonlinear *P-E*

Report Documentation Page

Form Approved
OMB No. 0704-0188

1. REPORT DATE	2. REPORT TYPE	3. DATES COVERED
2006		**00-00-2006 to 00-00-2006**

4. TITLE AND SUBTITLE	5a. CONTRACT NUMBER
Low-Voltage Ferroelectric Phase Shifters From L- to C-Band	5b. GRANT NUMBER
	5c. PROGRAM ELEMENT NUMBER
6. AUTHOR(S)	5d. PROJECT NUMBER
	5e. TASK NUMBER
	5f. WORK UNIT NUMBER
7. PERFORMING ORGANIZATION NAME(S) AND ADDRESS(ES) **Georgia Institute of Technology,School of Electrical and Computer Engineering,Atlanta,GA,30332**	8. PERFORMING ORGANIZATION REPORT NUMBER
9. SPONSORING/MONITORING AGENCY NAME(S) AND ADDRESS(ES)	10. SPONSOR/MONITOR'S ACRONYM(S)
	11. SPONSOR/MONITOR'S REPORT NUMBER(S)

12. DISTRIBUTION/AVAILABILITY STATEMENT
Approved for public release; distribution unlimited

13. SUPPLEMENTARY NOTES
The original document contains color images.

14. ABSTRACT

15. SUBJECT TERMS

16. SECURITY CLASSIFICATION OF:			17. LIMITATION OF ABSTRACT	18. NUMBER OF PAGES	19a. NAME OF RESPONSIBLE PERSON
a. REPORT	b. ABSTRACT	c. THIS PAGE			
unclassified	**unclassified**	**unclassified**		**8**	

characteristic. While this nonlinearity would be undesirable for fixed capacitor applications, it is the enabling mechanism for tuning ε_r, and thus realizing tunable capacitors.

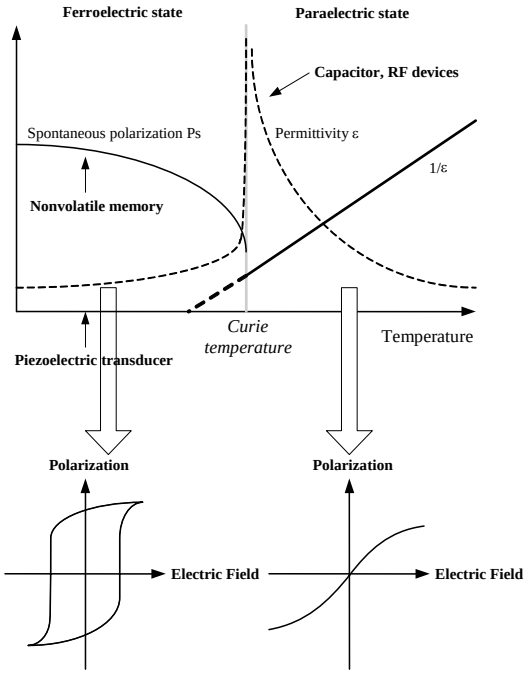

Figure 2: Polarization in ferroelectric and paraelectric states (after [2]).

III. BST VARACTOR DEVICES

The attractiveness of BST and other ferroelectric materials have encouraged many researchers to develop tunable capacitors, or varactors, using microelectronic fabrication techniques. Researchers at Georgia Tech, in collaboration with nGimat have developed interdigital capacitors (IDCs) for use in phase-shifter circuits for phased-array applications [3-7]. Figure 3 shows an example of an IDC device. IDCs have the advantage over parallel plate capacitor in that the capacitance values may be completely controlled by metallization patterns on one thick metal layer. We chose to use copper metal for obtaining high *Q* in both the IDCs, and spiral inductors that are integrated in the same process. Figure 4 shows a summary of performance of the tunable IDC. Figure 5 shows typical values of *Q* that may be obtained over a range of bias. While values of *Q* from 10 to 100 may be too low for narrow bandwidth, low loss filter applications, they are inline with traditional semiconductor diode varactor *Q's*, and are acceptable for medium loss applications. It should be noted that improvement of *Q* may be afforded at the expense of reduced tunability.

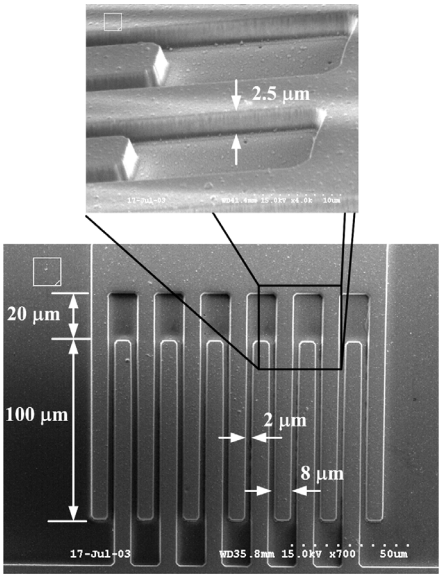

Figure 3: SEM image of the fabricated interdigital capacitor. The spacing of the capacitor fingers is 2 μm.

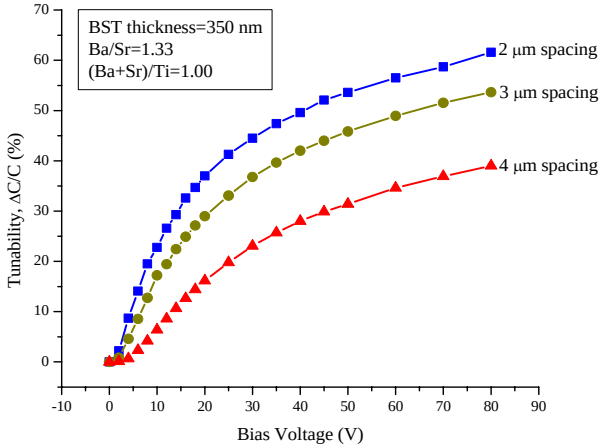

Figure 4: Tunability ($\Delta C/C_{max}$) of a BST IDC as a function of bias voltage at 2.4 GHz

Another characteristic of the BST IDCs that may be unattractive for some system level applications is the high bias voltages required. However, these high voltages can be an advantage when considering the nonlinear distortion produced by the RF voltage varying the

capacitance. Like semiconductor varactors, a lower tuning voltage necessarily implies increased intermodulation distortion (IMD) and total harmonic distortion (THD) performance [8].

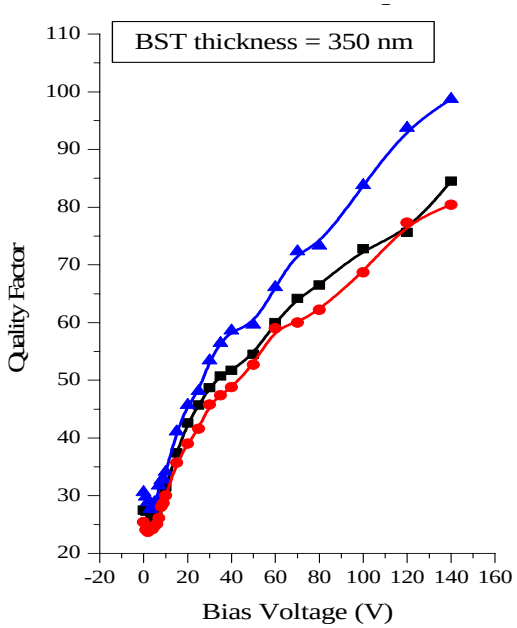

Figure 5: Quality Factor (Q) vs. bias for several BST IDCs.

Recently, BST IDC device structures have been developed that allow lower voltage operation, yet still maintain low distortion, high tunability, and other attractive features of the materials [9]. The devices utilize a separate bias IDC formed using a very thin, highly resistive layer of material. Figure 6 (a) illustrates the architecture of the low-voltage bias structure and its relationship to the RF IDC. Because the bias materials deposited in a very thin layer, bias electrodes may be placed in very close proximity, allowing highly concentrated *E*-fields produced by a low applied DC voltage. In addition, the RF fields do not interact with the highly resistive materials, as they are effectively shorted out by the high ε_r of the BST. Therefore, high-*Q* is maintained for the RF capacitor. Figure 6 (b) shows a photograph of the device, and Figure 6 (c) shows that high 3rd order input intercept points (IIP_3) may be obtained using the highly resistive bias structure. Both BST and the thin resistive layers were grown using nGimat's CCVD process [10].

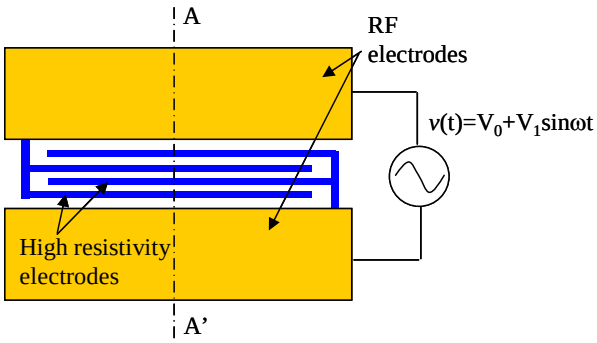

(a)

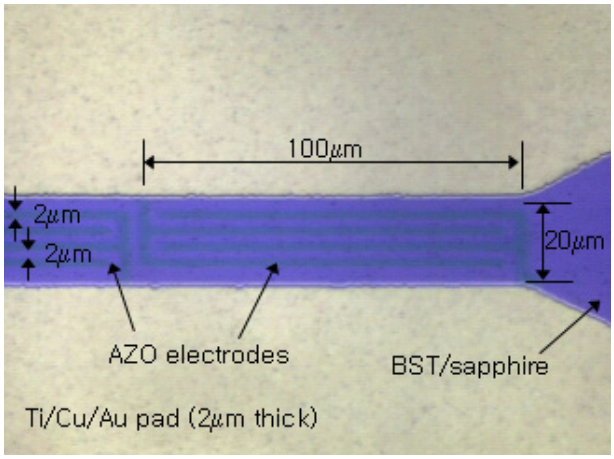

(b)

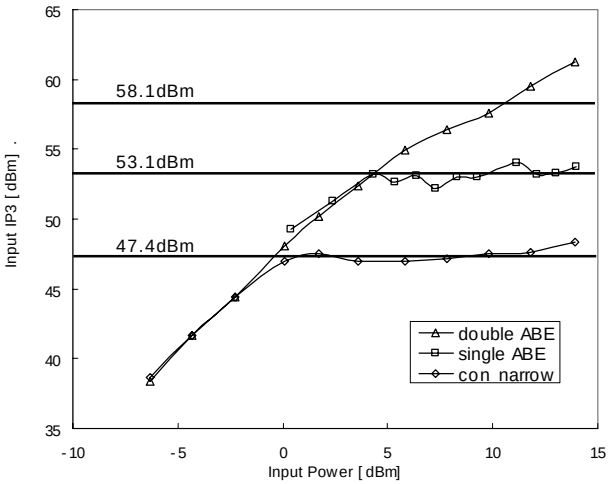

(c)

Figure 6: a) Illustration of low-voltage IDC, b) Microphotograph of a test device, and c) Measured IIP_3 of the low-voltage IDC.

IV. BST PHASE SHIFTER DESIGN

Using the BST IDCs that we developed, we have integrated these with lumped element inductors to realize continuously variable phase shifter circuits over a range of frequency. Several circuit architectures were considered. Reflection type phase shifters have the advantage of good VSWR over large bandwidths [4]. However, we found that the loss of the coupler that is necessary to realize this architecture contributed too heavily to the overall loss of the phase shifter. In addition, the coupler, being a distributed transmission line element, used a great deal of die space at lower frequencies. We abandoned this approach in favor an all-pass network (APN) filter architecture that utilizes only lumped elements, and avoids the coupler losses associated with reflection type phase shifters.

Figure 7 shows the equivalent circuit of the APN. While the circuit is all lumped elements, the *L-C* sections may be considered equivalent to a transmission line of characteristic impedance $Z_0 = \sqrt{L_1 / C_1}$.

As illustrated in Figure 7 (a) and 7 (b), the two lines may be considered to be coupled to one another by with even and odd mode reflection coefficients of

$$\Gamma_e = \frac{Z_{in}^e - Z_0}{Z_{in}^e + Z_0}, \qquad \text{(Eq. 1a)}$$

and

$$\Gamma_o = \frac{Z_{in}^o - Z_0}{Z_{in}^o + Z_0}, \qquad \text{(Eq. 1b)}$$

where

$$Z_{in}^e = j\omega(L_1 - 1/\, j\omega C_1), \qquad \text{(Eq. 2a)}$$

and

$$Z_{in}^o = (L_1 / C_1)/[j(\omega L_1 - 1/\omega C_1)]. \qquad \text{(Eq. 2b)}$$

The reflection coefficients as seen at either input of the APN may be given as

$$S_{11} = S_{22} = \frac{1}{2}(\Gamma_e + \Gamma_o) \qquad \text{(Eq. 3)}$$

Note that the return loss on either port is zero only if $Z_0 = \sqrt{L_1 / C_1}$. Likewise, the transmission through the APN is found to be

$$S_{21} = S_{12} = \frac{1}{2}(\Gamma_e - \Gamma_o) \qquad \text{(Eq. 4)}$$

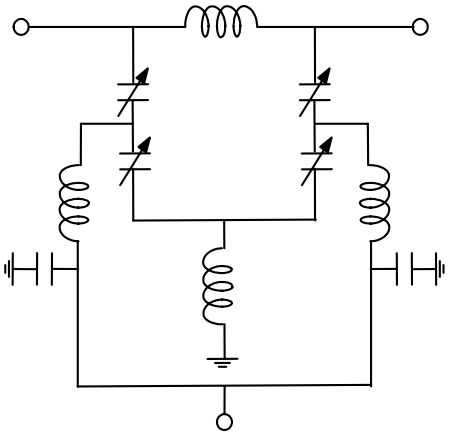

(a)

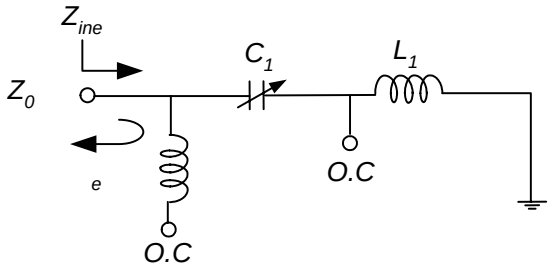

(b)

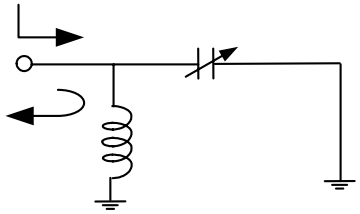

(c)

Figure 7: a) Schematic of all-pass phase shifter network, b) Even mode analysis, and c) Odd mode analysis.

From Eq. 3 and Eq. 4, it is clear that to achieve optimum return loss and insertion loss, the condition must be met that $Z_0 = \sqrt{L_1 / C_1}$ over the operating bandwidth. Because only tunable capacitors are available, it is necessary to accept some degradation in return loss in order to use fixed inductors. It was found that bandwidths exceeding 30% of center frequency are achievable at VSWRs less than 2:1. The element values were also optimized to insure minimal variation over temperature [11].

Early prototypes of the BST phase shifters utilized wire bonding and conventional packaging techniques. However, because the wire bond inductances led to variations in device performance, flip-chip packaging was pursued. Figure 8 shows a bottom view photograph of a typical flip-chip mounted BST phase shifter. The die size of the device shown below is less than .080 in. x .080 in.

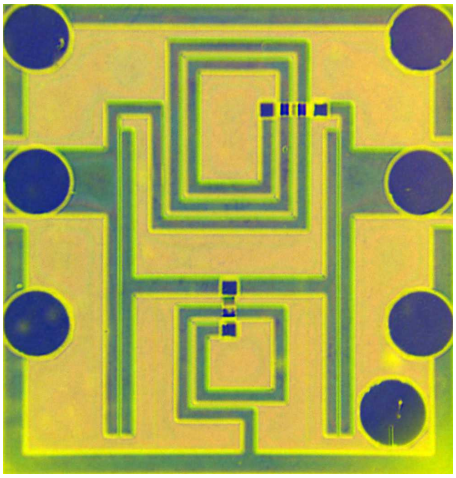

Figure 8: Photograph of an all pass network flip-chip BST phase shifter.

The same basic APN network was used to develop a family of commercial products now available at nGimat, Inc. Table I lists the frequency ranges and applications of various models. Figure 9 shows the swept response of a typical device. It is seen that the insertion loss is held to less than 2 dB over the usable bandwidth. The differential phase shift is over 100° of the bandwidth of operation. Multiple sections may be cascaded for higher differential phase shift values.

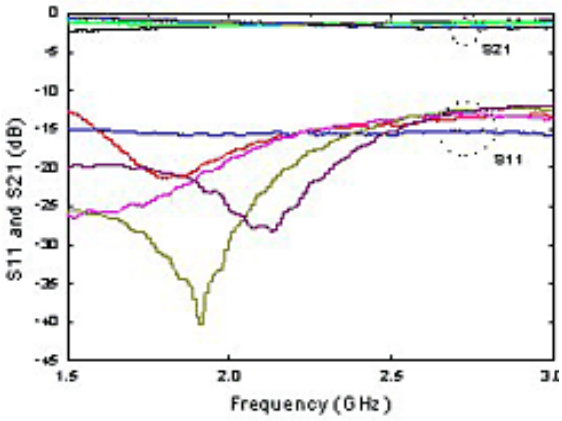

(a)

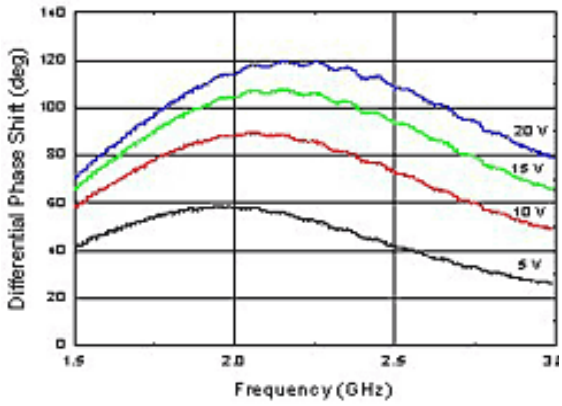

(b)

Figure 9: Typical performance of APN phase shifters. (a) Return loss, and (b)

TABLE I: NGIMAT BST PHASE SHIFTER PRODUCTS AND APPLICATIONS

Model Number	Freq. Range	Application
*n*PS0712	0.7 to 1.2 GHz	Nextel, US Cellular, GSM, 900MHz ISM, Paging, L-band Radar
*n*PS1217	1.2 to 1.7 GHz	GPS, Sirius/XM Radio
*n*PS1726	1.7 to 2.6 GHz	PCS, 3G UMTS, 802.11 b/g/n WLAN, WiBro, Bluetooth
*n*PS2538	2.5 to 3.8 GHz	MMDS, WiMax
*n*PS3756	3.7 to 5.6 GHz	Public Safety Radio, C-band satellite (Rx), NII
*n*PS4771	4.7 to 7.1 GHz	Public Safety Radio, C-band satellite (Tx)
*n*PS4060	4.0 to 6.0 GHz	802.11a, Point-to-point

V. A Phased Array Antenna using BST Phase Shifters

In order to illustrate the utility of BST phase shifters an interference mitigation system for 802.11g wireless local area network (WLAN) was designed, fabricated and tested [12]. Such a system may be implemented using phased array antennas. While high antenna directionality is not necessarily desirable in mobile communication systems that receive signals from multiple paths, it is sometimes beneficial to null out an interfering signal that emanates from a specific line-of-sight (LoS) direction. A two element phased-array can perform such an adaptive nulling operation without a significant loss of received signal strength. In addition, it only requires that each element have 180° of phase shift, thus minimizing insertion loss if the same antenna is used in transmit mode.

Figure 10 shows a photograph of the two element beam forming network fabricated using early prototypes of the BST phase shifters. Each phase shifter chip consisted of a two-section APN, with over 200° of phase shift from 2.4-2.45 GHz. It should be noted that these early prototypes did not use the low voltage bias structures previously described. As a result, more than half the PCB space was used for a high voltage power supply to bias the phase shifters. Because the flip-chip process had not yet been developed for these prototypes, the BST phase shifters were packaged in a conventional leadless chip carrier (LLC) ceramic package. Two inverted-F type surface mount antennas were assembled on a separate PCB (not shown), and connected to the BFN using coaxial cables via SMA connectors. The input was connected to an external antenna port on the WLAN card. The beam forming network was adaptively controlled using the parallel port of the laptop PC connected to the WLAN card.

Antenna patterns of the two-element array were measured at 2.4 GHz using an outdoor measurement range. These are shown in Figure 11 and are compared to pattern simulations. Discrepancies between measured and simulated data are likely due to antenna mounting issues not considered in the model. The data shows that nulls of more than 20-25 dB may be obtained in certain directions, while broad beams are maintained to receive the incoming multipath signals.

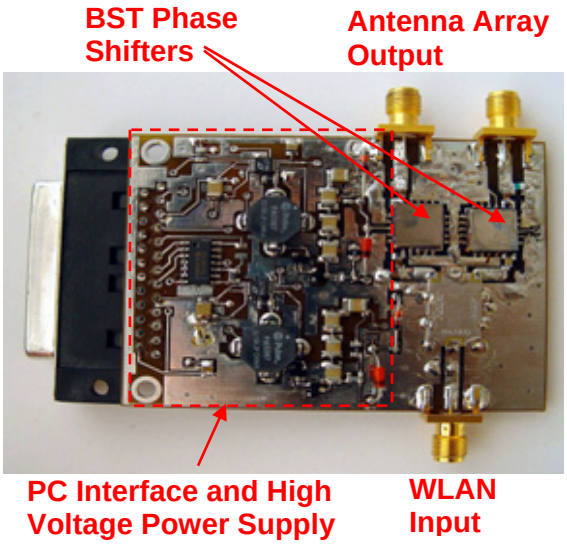

Figure 10: Photograph of a two-element beam forming network realized using BST phase shifters. Note: Early prototypes of the BST phase shifter were packaged conventionally, and did not contain the low-voltage bias structure.

A system level test was performed to ascertain the benefits of the adaptive nulling system as compared to the conventional switched diversity system currently employed on most WLAN devices. Interference signals at various levels were directed at the laptop computer attached to the WLAN card as it was receiving data from an access point that was not within line-of-sight to the phased array antenna. It is seen that the adaptive nulling afforded by the BST phase shifters achieves a throughput of 350-375 kByte/sec. This is approximately equal to the throughput of the WLAN card alone until the interference level is increased above -15 dBm (at the source of its transmission). Above this interference level, the throughput rapidly degrades for the conventional switched diversity WLAN antenna, while the adaptive nulling network is able to improve the signal-to-noise ratio (SNR) to maintain full throughput at up to 0 dBm interference level. Though the addition of the phased array antenna increased the insertion loss in transmit mode, no degradation in system performance was noted.

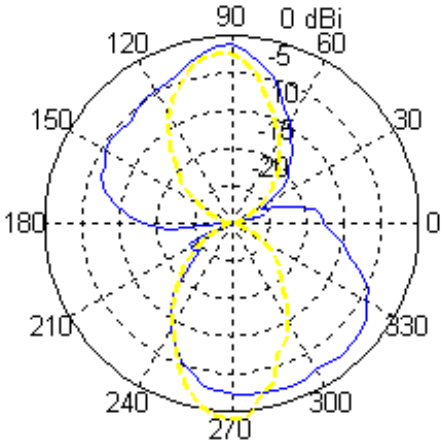

(a)

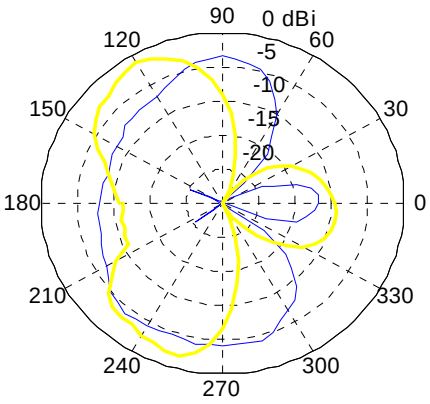

(b)

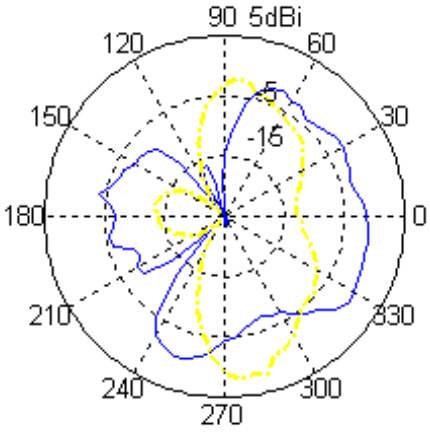

(c)

Figure 11: Measured antenna patterns for the two-element array (blue = measured, yellow = simulated (a) $\Delta\phi$ = 0°, (b) $\Delta\phi$ = 90°, and (c) $\Delta\phi$ = 30°.

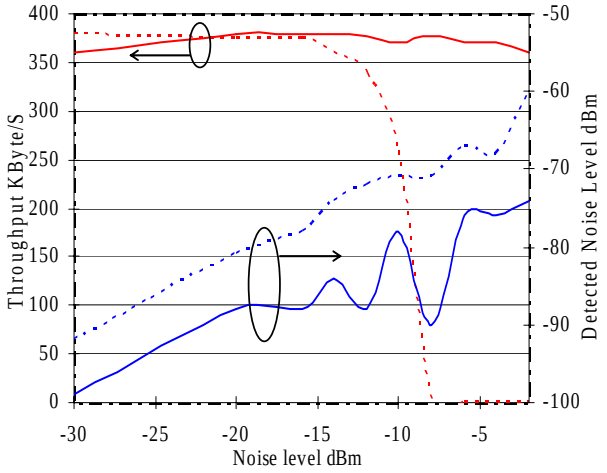

Figure 12: WLAN performance without (dashed line) and with (solid line) BST phased array antenna.

VI. Summary and Conclusions

This paper has presented the design, fabrication, and test results of a family of lumped-element, barium strontium titanate (BST) based phase shifters that cover frequency bands ranging from 700 MHz to 6 GHz. A minimum phase shift of 90 degrees was achieved over bandwidths exceeding 30% of the center frequency. They show insertion loss of <2 dB, and return loss of >13 dB, and may be continuously tuned with control voltages of 20 V or less. The input third-order intercept points (IIP_3) of all products are greater than 30 dBm over the range of control voltage. The flip-chip mounted chips are all sized less than 0.080 in. x 0.080 in. Using early prototypes of the BST phase shifters, a two-element 2.4 GHz phased-array antenna was fabricated and tested in conjunction with an off-the-shelf wireless LAN card. Null depths exceeding 20 dB were obtained by adjusting the BST phase shifters. Using an adaptive nulling algorithm to steer the phased array antenna, high data throughput was maintained at interference levels significantly beyond those that caused the WLAN connection to fail.

Acknowledgement

This work was supported in part by U.S. Air Force SBIR contract number F33615-01-M-1950. Other parts of this work were supported by NSF SBIR grant DMI-0349729.

REFERENCES

[1] F. Jona and G. Shirane, *Ferroelectric Crystals*, New York: Dover Press, 1993.

[2] K. Uchino, *Ferroelectric Devices*, Marcel Dekker, Inc., 2000.

[3] D. S. Kim, Y. S. Choi, M. Ahn, M. G. Allen, J. S. Kenney, and D. Kiesling, "S-Band Ferroelectric Phase Shifters with Continuous 180° and 360° Phase Shift Range," in *2002 Asia Pacific Microwave Symp. Dig.*, Nov. 18-20, 2002.

[4] D. S. Kim, Y. S. Choi, M. G. Allen, J. S. Kenney, and D. Kiesling, "A Wide Bandwidth Monolithic BST Reflection-Type Phase Shifter Using a Coplanar Waveguide Lange Coupler," *IEEE Trans. Microwave Theory and Tech.*, Vol. 50, No. 12, pp. 2903-9, Dec. 2002.

[5] D. S. Kim, Y. S. Choi, M. G. Allen, and J. S. Kenney, "Monolithic 180° and 360° Analog Phase Shifters Based on Based on BST Coated Substrate," *IEICE Trans. Elect.*, Vol. E-86-8, No. 8, pp. 1607-12, Aug. 2003.

[6] D. S. Kim and J. S. Kenney, "Tunable $Ba_{0.6}Sr_{0.4}TiO_3$ Interdigital Capacitors for Microwave Applications," in *Proc. 2003 Asia-Pacific Microwave Conf.*, Nov. 4-7, 2003, Seoul, South Korea.

[7] D. S. Kim, Y. S. Choi, M. Ahn, M. G. Allen, J. S. Kenney, and P. Marry, "2.4 GHz Continuously Variable Ferroelectric Phase Shifters Using All-Pass Networks," *IEEE Microwave and Wireless Component Lett.*, Vol. 13, No. 10, pp. 434-36, Oct. 2003.

[8] D. S. Kim and J. S. Kenney, "Experimental Investigations of Intermodulation Distortion in Tunable Ferroelectric Phase Shifters," *IEICE Trans. Elect.*, Vol. E85, No. 1, Dec. 2005.

[9] Y. K. Yoon, D. S. Kim, M. G. Allen, A. Hunt, and J. S. Kenney, "A Reduced Intermodulation Distortion Tunable Ferroelectric Capacitor: Architecture and Demonstration," *IEEE Trans. Microwave Theory and Tech.*, Vol. 51, No. 12, pp. 2568-76, Dec. 2003.

[10] A. Hunt, B. Carter and J Cochran. "Combustion Chemical Vapor Deposition of Films and Coatings," US Patent # 5,652,021, 1997.

[11] D. S. Kim, S. S. Je, J. S. Kenney, and P. Marry, "Design of Ferroelectric Phase Shifters for Minimum Performance Variation over Temperature," *2004 IEEE MTT-S Int. Microwave Symp. Dig.*, June 6-10, 2004, Ft. Worth, TX. pp. 257-60.

[12] M. Ahn, D. Kim, and J. S. Kenney, "Throughput Improvement in Interference Limited Multipath Environments using a Ferroelectric Smart Antenna for IEEE 802.11b WLAN," *Proc. 2004 Radio and Wireless Conf.*, Sep. 19-22, 2004, Atlanta, GA, pp. 411-14.